Impact of the spread-spectrum technique on the higher-order harmonics and radiated emissions of a synchronous buck converter

Impact of the Spread-Spectrum Technique on the Higher-Order Harmonics and Radiated Emissions of a Synchronous Buck Converter

Raul Blecic*, Fabio Pareschi†‡, Josip Bacmaga*, Riccardo Rovatti§‡, Gianluca Setti¶‡, Adrijan Baric*
* University of Zagreb Faculty of Electrical Engineering and Computing, Unska 3, 10000 Zagreb, Croatia
† Engineering Department in Ferrara (ENDIF), University of Ferrara, 44100 Ferrara, Italy
‡ Advanced Research Center on Electronic Systems (ARCES), University of Bologna, 40125 Bologna, Italy
§ Department of Electrical, Electronic, and Information Engineering, University of Bologna, 40136 Bologna, Italy
¶ Department of Electronics and Telecommunications, Politecnico di Torino, 10129 Torino, Italy
Tel: +385 (0)1 6129547, fax: +385 (0)1 6129653, e-mail: raul.blecic@fer.hr

***Abstract*—Synchronous buck converters generate electromagnetic emissions which may violate the limits specified in the regulations. Spread-spectrum is an effective technique for reducing the electromagnetic interference of switching devices. The reduction of the magnitude of the first harmonic by the spread-spectrum technique is mainly in focus in the literature. In this paper, the impact on the higher-order harmonics and on the radiated emissions is analyzed. A non-regulated synchronous buck converter is used as a device under test. The radiated emissions of the converter are calculated from the measurements performed by a transverse electromagnetic cell and a hybrid coupler. The measurements are performed for different values of the parameters of the spread-spectrum technique and a reduction of up to 5.7 dB is obtained.**

***Index Terms*—electromagnetic compatibility, electromagnetic interference, power conversion, switched-mode power supply, transverse electromagnetic cell.**

I. Introduction

Synchronous buck converters are sources of electromagnetic (EM) interference which is a result of the switching operation and high $\mathrm{d}i/\mathrm{d}t$ and $\mathrm{d}v/\mathrm{d}t$ [1], [2]. The levels of the generated EM interference may violate the limits specified in the regulations [3].

Spread-spectrum has been employed recently as an effective technique for reducing the EM interference of switching devices [4]–[8]. The focus in these papers is placed on reducing the magnitude of the first harmonic. However, the first harmonic may not be the only one which violates the limits. For example, the maximum value of the radiated emissions of synchronous buck converters typically occurs in the frequency range from 50 to 300 MHz [9], although the switching frequency (i.e. the frequency of the first harmonic) is typically not larger than a few MHz.

In this paper, the impact of the spread-spectrum technique on the higher-order harmonics and on the radiated emissions of a non-regulated synchronous buck converter is analyzed. The spread-spectrum technique is applied to the control signal of the converter. The radiated emissions of the converter are calculated from the equivalent model of dipole moments. The dipole moments are extracted from the measurements performed by a transverse electromagnetic (TEM) cell and a hybrid coupler [10], [11]. The measurements are performed for different parameters of the spread-spectrum technique.

Section II describes the principle of operation of the spread-spectrum technique and its impact on the higher-order harmonics. Section III presents the impact of applying the spread-spectrum technique to the radiated emissions of a synchronous buck converter. Section IV concludes the paper.

II. Spread-Spectrum Technique

A. Principle of Operation

Spread-spectrum techniques aim at spreading the energy of a narrowband signal into its adjacent band by introducing new spectral components in the frequency spectrum. This is beneficial from the EM compatibility point-of-view since the magnitudes of all resulting components are smaller than the magnitude of the corresponding harmonic before the technique is applied because the total energy of the signal is conserved.

Among different spread-spectrum techniques, this paper considers the frequency modulation (FM) of a control signal. The parameters of the FM are the modulation frequency f_m, frequency deviation Δf and modulation function $\mathrm{f}(f_m)$. The impact of spreading the spectrum of the harmonics is also determined by all three parameters. Most of the energy of the signal is spread into the Carson's bandwidth defined by Δf [12]. The modulation function defines the shape of the spectrum, while f_m defines the separation of the spectral components. Increasing Δf or decreasing f_m introduces more spectral components within the Carson's bandwidth, thus reducing the average magnitude of these components. The modulation index m combines the two parameters as:

$$m = \Delta f / f_m. \tag{1}$$

B. Impact of the Spread-Spectrum Technique on Higher-Order Harmonics

By applying the FM to the converter control signal (assumed to be a clock signal at the frequency f_{sw}), the result is the same as if applying the FM with different modulation parameters

to each harmonic. In detail, all harmonics are modulated by the same modulation frequency f_m, while the frequency deviation of the n-th harmonic is n times larger than Δf of the fundamental frequency. Let the apparent frequency deviation Δf_n be defined as the frequency deviation of the n-th harmonic, calculated as:

$$\Delta f_n = n \cdot \Delta f. \tag{2}$$

The apparent modulation index, i.e. the modulation index seen by the n-th harmonic, can be calculated as:

$$m_n = \frac{\Delta f_n}{f_m} = \frac{n \cdot \Delta f}{f_m} = n \cdot m. \tag{3}$$

The choice of Δf is typically a trade-off. High values maximize the impact of the spread-spectrum technique. However, the upper value of Δf is always limited by the impact of the spread-spectrum technique on the other characteristics of the switching device which can be tolerated for a specific application, such as the efficiency and the ripple of the output voltage in the case of synchronous buck converters.

Furthermore, increasing Δf leads to the overlap of the bands where the energy of higher-order harmonics is spread, with a possible reduction in the spread spectrum effectiveness. This occurs because the apparent frequency deviation Δf_n increases linearly with the index of the harmonic, while the separation of two adjacent harmonics is fixed and equal to f_{sw}. Referring to the generic n-th harmonic, the overlap may occur both in the upper and lower frequency bands. The overlap of the n-th harmonic, some lower n_1-th harmonic and, consequently, of all harmonics in between occurs if the sum of the apparent frequency deviation is larger than the distance between the two harmonics. The expression can be written as:

$$n \cdot \Delta f + n_1 \cdot \Delta f \geq (n - n_1) \cdot f_{sw}. \tag{4}$$

Equivalently, the overlap of the n-th, some higher n_2-th harmonic and of all harmonics in between occurs if:

$$n \cdot \Delta f + n_2 \cdot \Delta f \geq (n_2 - n) \cdot f_{sw}. \tag{5}$$

Re-arranging (4) and (5) allows to compute the index of the lowest overlapped harmonic n^{low} and that of the highest overlapped harmonic n^{up} for a given n, Δf and f_{sw}:

$$n^{low} = \left\lceil n \cdot \frac{f_{sw} - \Delta f}{f_{sw} + \Delta f} \right\rceil, \tag{6}$$

$$n^{up} = \left\lfloor n \cdot \frac{f_{sw} + \Delta f}{f_{sw} - \Delta f} \right\rfloor. \tag{7}$$

III. Synchronous Buck Converter

A. Designed Converter

The converter analyzed in this paper is a non-regulated synchronous buck converter based on the device NCP5369 [13]. The simplified schematic of a synchronous buck converter is shown in Fig. 1. The device NCP5369 integrates a low-side (LS) field effect transistor (FET), a high-side (HS) FET, a digital control circuitry and a driving circuitry in one 40-pin package. The control signal (i.e. the pulse width modulation (PWM) signal) is generated by a signal generator and it is applied to the PWM input pin of the device.

The converter is designed on a 1.55-mm thick 2-layer printed circuit board (PCB). All components are placed on the top layer. The bottom layer is a solid ground plane. The input decoupling network consists of four (1 µF, 10 µF, 22 µF and 100 µF) multilayer ceramic capacitors (MLCCs). The output filter consists of one 1-µH inductor and three MLCCs (1 µF, 10 µF, 22 µF). The top view of the PCB is shown in Fig. 2.

The red circle in Fig. 2 indicates the position of a radiating loop which is typically the dominant source of the radiated emissions of synchronous buck converters [9], [14]. The radiating loop is a consequence of the resonance in the input decoupling network. The resonance occurs between the capacitance of the FET in the off-state and the parasitic inductance of the input decoupling network L_{IDN} [9], [14].

The time-domain measurements are performed to validate the operation of the converter. The voltage of the switching node in the steady-state operation measured by a 300-MHz bandwidth oscilloscope is shown in Fig. 3. The efficiency of the converter is calculated from the measured data as:

$$\eta = \frac{V_{OUT} \cdot I_{OUT}}{V_{IN} \cdot I_{IN}}. \tag{8}$$

The efficiency as a function of the switching frequency and for three values of the input voltage while keeping the output voltage fixed at 1.8 V is shown in Fig. 4. The peak efficiency of 93.1% is obtained.

The spread-spectrum technique is applied to the converter under the test conditions as follows. The converter converts the input voltage of 6 V into the output voltage of 1.8 V. The output current is set to 3 A by the electronic load. The switching frequency is set to 1.25 MHz. Under these conditions, the measured efficiency is 89.1%.

B. Calculation of the Radiated Emission

The analyzed converter is assumed to be an electrically small antenna. Its radiation characteristics are modelled by 5 collocated orthogonal dipole moments (3 magnetic and 2 electric, the third electric dipole moment cannot be measured by the measurement setup because of the dimensions of the TEM cell and PCB). The dipole moments are extracted from the measurements performed by the TEM cell and hybrid coupler [10], [11]. The schematic representation of the measurement setup is shown in Fig. 5. The TEM cell is used as

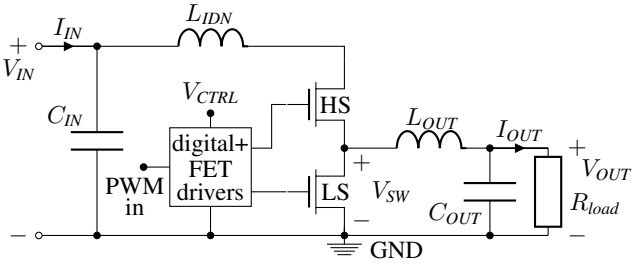

Fig. 1. Simplified schematic of a synchronous buck converter.

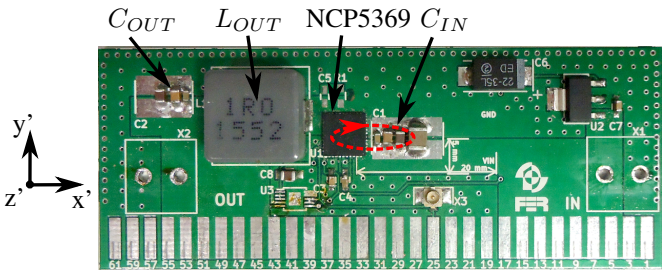

Fig. 2. Top view of the PCB. The red circle indicates the position of the radiating loop which is typically the dominant source of the radiated emissions of synchronous buck converters.

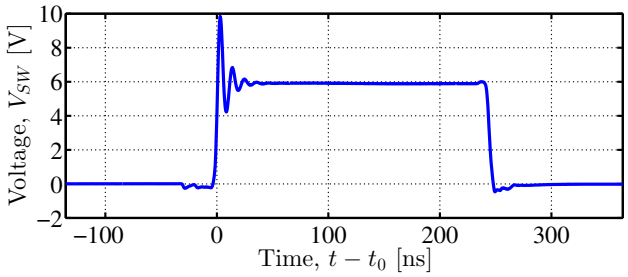

Fig. 3. Voltage of the switching node in the steady-state operation ($t_0 >> 1/f_{sw}$). A resonance, which is typically the dominant source of the radiated emissions, can be seen at the rising edge.

a near-field sensor of the generated fields, while the hybrid coupler is used to separate the contributions of the electric and magnetic dipole moments.

Positioning the converter in the TEM cell as shown in Fig. 5 allows to extract one electric and one magnetic dipole moment of the converter. The converter is rotated inside the TEM cell in three orthogonal dipole positions to extract other dipole moments. The modular board system, which allows to position the converters inside the TEM cell in different positions, and the procedure for calculating the radiated fields from the extracted dipole moments are described in [10], [11].

C. Impact of the Spread-Spectrum Technique

The analysis of the impact of the spread-spectrum technique on the radiated emissions of the converter is performed by applying the modulation to the control signal. The modulation

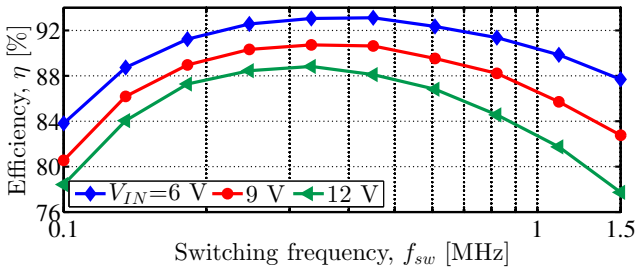

Fig. 4. Measured efficiency of the designed converter as a function of the switching frequency and for three values of the input voltage while keeping the output voltage fixed at 1.8 V.

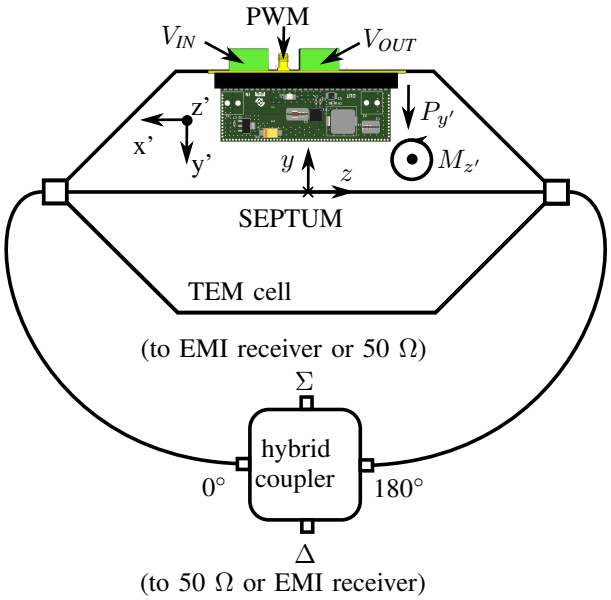

Fig. 5. Schematic representation of the measurement setup for the extraction of the dipole moments of the measured converter.

TABLE I
PARAMETERS OF THE APPLIED MODULATION.

Description	Parameter	Value
Modulation function	f(f_m)	triangular
Modulation index	m	1, 2, 5, 10, 20, 50, 100
Frequency deviation	Δf [kHz]	50, 100, 200

function f(f_m) is generated internally by the same signal generator that generates the control signal. The parameters of the applied modulation are given in Table I. The parameters f_m and Δf are varied in the same range of values as in [7], while only the triangular modulation function is considered for simplicity.

The measurements of the coupling to the TEM cell are performed by an EMI receiver and a peak detector. These measurements are used to calculate the radiated emissions of the converter at a distance of 10 m. The calculated radiated emissions before and after applying the spread-spectrum technique are shown in Fig. 6. The emissions after applying the spread-spectrum technique are shown for the parameters of the modulation which give the largest reduction ($\Delta f = 200$ kHz, $m = 50$). The maximum value of the radiated emissions before applying the spread-spectrum technique is 13.8 dB µV/m at 121.25 MHz, i.e. at the 97th harmonic. The impact of the spread-spectrum technique is evaluated as the difference of the maximum value before and after applying the spread-spectrum technique. The impact for different parameters of the modulation is shown in Fig. 7.

The maximum reduction of the peak level of the first harmonic in [7] is approximately 7, 9 and 11 dB for Δf equal to 50, 100 and 200 kHz, respectively. The level of reduction increases with Δf. Here, the maximum reduction is approximately 6 dB for all three values of Δf. Although

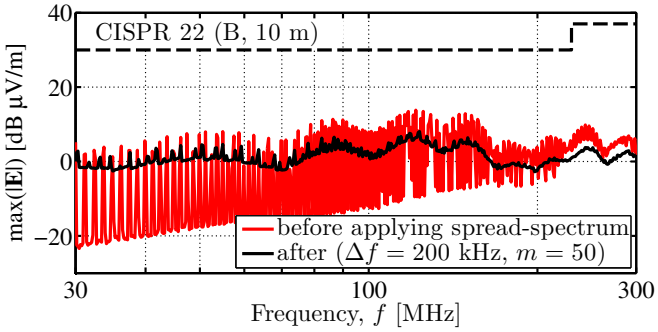

Fig. 6. Comparison of the spectrum before and after applying the spread-spectrum technique.

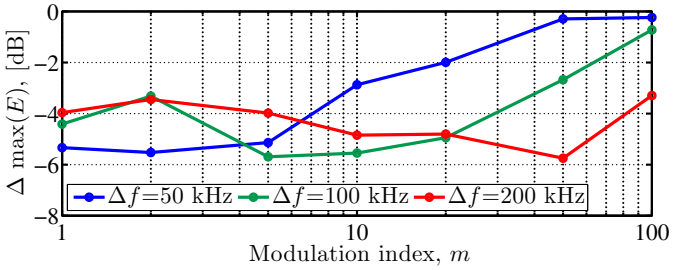

Fig. 7. The impact for different parameters of the modulation evaluated as the difference of the maximum value before and after applying the spread-spectrum technique.

the apparent modulation index is very large in these cases, the reduction is smaller than in [7] because of two reasons.

The first one is the overlap of the higher-order harmonics, which limits the effectiveness of the spread-spectrum technique. The indexes of the lowest and highest harmonics overlapped with the 97th harmonic for Δf of 50, 100 and 200 kHz calculated by (6) and (7) are given in Table II.

The second reason is a different resolution bandwidth (RBW) used for the measurements of conducted and radiated emissions. The RBW is equal to 9 kHz for the conducted, while it is equal to 120 kHz for the radiated emissions [3]. The resolution bandwidth defines the separation of two harmonics which can be resolved by the EMI receiver. In terms of the spread-spectrum, it determines how effective the spread-spectrum can potentially be. A smaller RBW means that more spectral components can be used to spread the energy of the harmonic. Considering the values of the RBW, the spread-spectrum technique is potentially more effective in reducing the conducted than in reducing the radiated emissions.

TABLE II
INDEXES OF THE HARMONICS OVERLAPPED WITH THE 97TH HARMONIC ($n = 97$).

Δf [kHz]	Δf_n [kHz]	n^{low}	n^{up}	Number of overlapped harmonics calculated as $n^{up} - n^{low} + 1$
50	4850	90	105	16
100	9700	83	113	31
200	19400	71	133	63

Despite this and despite the fact that 63 harmonics are overlapped (for Δf = 200 kHz), the spread-spectrum technique reduces the radiated emission of the designed synchronous buck converter by up to 5.7 dB.

IV. Conclusion

The impact of the spread-spectrum technique on the radiated emissions of a synchronous buck converter is analyzed. The converter operates at the switching frequency of 1.25 MHz. The maximum value of the radiated emissions occurs at 121.25 MHz, which is the 97th harmonic. For the frequency deviation of 200 kHz, the 97th harmonic is overlapped with 62 adjacent harmonics. This limits the effectiveness of the spread-spectrum technique in reducing the radiated emissions. Despite the overlap, the reduction of up to 5.7 dB is obtained.

Acknowledgment

This work was supported in part by the Croatian Science Foundation (HRZZ) within the project "Advanced design methodology for switching dc–dc converters".

References

[1] F. L. Luo and H. Ye, "Investigation of EMI, EMS and EMC in power DC/DC converters," in *Proc. IEEE Int. Conf. on Power Electron. and Drive Systems (PEDS)*, vol. 1, Nov. 2003, pp. 572–577.
[2] Z. Li and D. Pommerenke, "EMI specifics of synchronous DC-DC buck converters," in *Proc. IEEE Int. Symp. Electromagn. Compat.*, vol. 3, 2005, pp. 711–714.
[3] C. Paul, *Introduction to Electromagnetic Compatibility*. Wiley, 2006.
[4] V. Subotskaya, K. Cherniak, K. Hoermaier, and B. Deutschmann, "Emission reduction with spread spectrum clocking for switched capacitor buck converter," in *IEEE International Symposium on Electromagnetic Compatibility and IEEE Asia-Pacific Symposium on Electromagnetic Compatibility (EMC/APEMC)*, May 2018, pp. 297–302.
[5] B. Auinger, B. Deutschmann, and G. Winkler, "Elimination of electromagnetic interference in communication channels by using spread spectrum techniques," in *International Symposium on Electromagnetic Compatibility (EMC EUROPE)*, Sept. 2017, pp. 1–6.
[6] B. Deutschmann, G. Winkler, and T. Karaca, "Emission reduction in Class D audio amplifiers by optimizing spread spectrum modulation," in *International Workshop on the Electromagnetic Compatibility of Integrated Circuits (EMC Compo)*, Nov. 2015, pp. 1–6.
[7] F. Pareschi, R. Rovatti, and G. Setti, "EMI Reduction via Spread Spectrum in DC/DC Converters: State of the Art, Optimization, and Tradeoffs," *IEEE Access*, vol. 3, pp. 2857–2874, 2015.
[8] F. Pareschi, G. Setti, R. Rovatti, and G. Frattini, "Practical Optimization of EMI Reduction in Spread Spectrum Clock Generators With Application to Switching DC/DC Converters," *IEEE Trans. on Power Electron.*, vol. 29, no. 9, pp. 4646–4657, Sept. 2014.
[9] A. Bhargava, D. Pommerenke, K. Kam, F. Centola, and C. W. Lam, "DC-DC Buck Converter EMI Reduction Using PCB Layout Modification," *IEEE Trans. Electromagn. Compat.*, vol. 53, no. 3, pp. 806–813, Aug. 2011.
[10] R. Blecic, H. Stimac, R. Gillon, B. Nauwelaers, and A. Baric, "Improved Estimation of Radiated Fields of Unintentional Radiators by Correction of the Impedance Mismatch Between a Transverse Electromagnetic Cell and a Hybrid Coupler," *IEEE Trans. Electromagn. Compat.*, 2017, doi:10.1109/TEMC.2017.2769021.
[11] R. Blecic, R. Gillon, B. Nauwelaers, and A. Baric, "EMC-Oriented Design of Output Stage of Synchronous Buck Converter," in *IEEE Int. Workshop on Electromagn. Compat. of Integrated Circuits (EMC Compo)*, July 2017.
[12] H. Black, *Modulation theory*. Van Nostrand, 1953.
[13] O. Semiconductor, *NCP5369 Integrated Driver and MOSFET, datasheet*, Apr. 2015.
[14] K. Kam, D. Pommerenke, F. Centola, C. wei Lam, and R. Steinfeld, "EMC guideline for synchronous buck converter design," in *Proc. IEEE Int. Symp. Electromagn. Compat.*, Aug. 2009, pp. 47–52.